PCCP

Sulfur addition to microwave activated CH_4/CO_2 gas mixtures used for diamond CVD: growth studies and gas phase investigations

James R. Petherbridge, Paul W. May,* Edward J. Crichton, Keith N. Rosser and Michael N. R. Ashfold

School of Chemistry, University of Bristol, Bristol, UK BS8 1TS. E-mail: paul.may@bris.ac.uk

Received 21st June 2002, Accepted 21st August 2002
First published as an Advance Article on the web 16th September 2002

Microwave plasma chemical vapour deposition (MPCVD) has been used to deposit diamond films with H_2S additions of 0–5000 ppm to a 51% CH_4/49% CO_2 plasma, with growth carried out for two different substrate temperatures (620 and 900 °C). Film morphology, growth rate and quality are all observed to deteriorate with increased H_2S addition, as investigated by scanning electron microscopy (SEM) and laser Raman spectroscopy (LRS). H_2S addition also appears to alter the resistivity of films, as measured by the four-point probe method, however X-ray photoelectron spectroscopy (XPS) revealed little incorporation of sulfur. The plasma chemistry leading to film deposition has been investigated using optical emission spectroscopy (OES), in which H_2S addition leads to a reduction in C_2* and CH* intensities. Molecular beam mass spectrometry (MBMS) measurements have detected a build-up in CS, CS_2, SO and SO_2 concentrations with addition of H_2S. Experimental results have been compared to CHEMKIN simulations of plasma chemistry and S-incorporation has been investigated in terms of the product of CHEMKIN predicted mole fractions of CH_3 and CS, $[CH_3] \times [CS]$.

I. Introduction

The many extreme physical and mechanical properties[1,2] of thin diamond films grown by chemical vapour deposition (CVD) have prompted interest in such films for use in electronic devices. CVD diamond films exhibiting p-type semiconductor properties are routinely grown by addition of B-containing gases to the standard CVD gas mixture (1% CH_4/H_2).[3,4] However, obtaining n-type semiconducting diamond films by CVD has proved more challenging, mainly due to the fact that potential donor atoms (*e.g.* N, P, O and As) are larger than carbon, discouraging incorporation into the diamond lattice. However, n-type conductivity has been reported by the method of sulfur ion implantation into CVD homoepitaxial diamond (100) films.[5] Furthermore, Sakaguchi *et al*[6–8] have reported that H_2S addition to a 1% CH_4/H_2 gas mixture during microwave plasma enhanced CVD (MPCVD) leads to the growth of semiconducting, homoepitaxial diamond films exhibiting n-type behaviour. Film growth rates were observed to decline with increased H_2S addition, however the quality of the films (as assessed *via* Raman spectroscopy) was found to be comparatively insensitive to changes in H_2S addition. Relatively high Hall mobilities (597 $cm^2 V^{-1} s^{-1}$) were measured[6] for films produced using H_2S doping levels of 50–100 ppm. Subsequent re-analysis of these samples[9] has raised some uncertainties with these results, however.

Experimental measurements of gas phase species concentrations present during the growth of sulfur doped CVD diamond films from H_2S have been reported by both our group[10,11] and others.[12] In the work of Sternschulte *et al*,[12] gas was sampled *via* a glass capillary tube at a point downstream from the microwave (MW) plasma, and was analysed by a quadrupole mass spectrometer. They showed that H_2S addition to a 1% CH_4/H_2 MW plasma caused a decrease in CH_3 concentrations leading to a decrease in diamond film growth rate, with the conclusion being that CH_4 and H_2S were reacting in the gas phase to form CS.

Studies within our own group[10,11] used molecular beam mass spectrometry (MBMS) to sample gas directly from the plasma, thus probing the gas phase chemistry with minimum perturbation from gas-surface reactions. We have used this powerful technique previously to obtain absolute mole fractions of the gas phase species present in both hot filament[13–16] and microwave systems[10,17,18] for a variety of gas mixtures and dopant gas additions. Our conclusions from measurements made of H_2S/1% CH_4/H_2 MW plasmas were in good agreement with those of Sternschulte *et al*,[12] and led us to propose a mechanism, based on the overall Reaction 1, for the coupling of C and S containing species in the gas phase to form CS and CS_2. This proposal was supported by simple thermodynamic arguments, while CS was suggested as a possible species responsible for S incorporation within the diamond lattice.

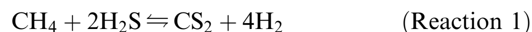

$$CH_4 + 2H_2S \rightleftharpoons CS_2 + 4H_2 \qquad \text{(Reaction 1)}$$

Computer simulations of the gas phase chemistry of H/C/S containing CVD gas mixtures have been carried out by Barber and Yarbrough.[19] They concluded that addition of CS_2 to the 1% CH_4/H_2 mixture caused a reduction in the gas phase concentration of hydrocarbons, leading (in conjunction with other proposed mechanisms) to the reduction in diamond film growth rates observed experimentally. Dandy[20] presented equilibrium calculations for $H_2S/CH_4/H_2$ gas mixtures and concluded that sulfur incorporation into the diamond lattice in such systems was *via* the SH radical. However, both of these studies were confined to equilibrium thermodynamic calculations, with the kinetics relevant to a CVD environment neglected. Our proposed S–C coupling mechanism (*i.e.* Reaction 1) has been validated by comparing the results of SENKIN kinetics calculations to previously published MBMS experimental measurements of species mole fractions, for H_2S/1% CH_4/H_2 gas mixtures.[10]

This journal is © The Owner Societies 2002

Sternschulte *et al* have suggested that a substrate temperature, T_{sub}, lower than that used during standard diamond CVD (900 °C), may influence the growth of S-doped diamond films.[12] Gas mixtures in the region of 50% CH_4/50% CO_2 have been shown to enable diamond growth at significantly lower temperatures than those required by the orthodox 1% CH_4/H_2 gas mixture.[21–23] No previous studies have investigated the effect of H_2S addition to a 51% CH_4/49% CO_2 gas mixture at various T_{sub}, from the perspective of either the deposited films or the gas phase chemistry. Here, we present such a study for additions of 0–5000 ppm H_2S, with deposition carried out at T_{sub} = 900 and 620 °C. Experimental MBMS measurements of plasma species are also compared with SENKIN predicted species mole fractions.

II. Experimental

(a) Growth experiments

Diamond deposition was performed using a 1.5 kW ASTeX-style 2.45 GHz microwave plasma CVD reactor.[17] The double-walled chamber was water cooled and contained a water-cooled Mo substrate holder. Experiments were carried out at two substrate temperatures, T_{sub}, 620 and 900 °C. For the 900 °C experiments, the Mo substrate holder was covered using a blank Si wafer, since it has been reported that Mo at such high temperatures possibly acts as a sink for gas phase S species, scavenging them and reacting to form solid MoS_2.[24] Substrates were placed on an alumina plate on top of this Si cover wafer, and were thus elevated about 1 mm into the plasma, enabling automatic heating of the substrate to ~900 °C (as measured by a two color optical pyrometer, emissivity setting = 1.0). Such substrate mounting was used in previous work using H_2S/1% CH_4/H_2 gas mixtures,[10] thus enabling direct comparisons of results obtained using both this, and the CH_4/CO_2 gas mixture used in the present work. Experiments using the lower substrate temperature were carried out with the substrate placed directly on the Mo substrate holder, thus allowing T_{sub} to be maintained at 620 °C using a substrate holder cooling system as reported previously.[25] The surface of the substrate holder not covered by the substrate was covered with Si wafers to prevent possible scavenging of sulfur as described above.

Films were deposited on undoped single crystal (100) silicon wafers (resistivity ~2.3×10^5 Ω cm), and had been manually pre-abraded with 1–3 μm diamond grit. The duration of deposition was 8 h at a pressure of 40 Torr with 1 kW applied microwave power. The feedstock gases used were CH_4 (99.999% purity), CO_2 (99.99% purity) and H_2S (99.5% purity). To obtain gas phase H_2S levels below 1000 ppm, a cylinder of 1% H_2S in CH_4 was employed, and further diluted by use of appropriate flow rate ratios regulated by mass flow controllers. Total gas flow was maintained at 100 sccm. At the conclusion of deposition the plasma was switched off, H_2S and CH_4 flows were shut off, and the substrate was cooled in a CO_2 atmosphere.

Films were examined by scanning electron microscopy (SEM, JEOL 5600LV instrument) to determine crystal morphology and thickness, and by 514.5 nm (Ar^+) laser Raman spectroscopy (LRS, Renishaw system 2000) to assess film quality. Film growth rates were calculated by dividing the SEM measured cross-sectional thickness by the deposition time of 8 h. Raman spectra were fitted using the Grams/32 computer program.[26] The procedure used a quadratic function to fit the underlying spectral background and Gaussian lineshapes to fit to the bands. The film quality, *i.e.* diamond content, was investigated by calculating a quality factor, Q. This is defined in terms of the integrated area of the diamond line, A_d, and the combined integrated areas of all the non-diamond Raman bands, A_n. If it is assumed that these non-diamond components are all amorphous carbon (which has a reported Raman cross section ~233 times larger than diamond at 514 nm), then Q can be defined as a percentage[27] as shown below:

$$Q = \frac{A_d}{A_d + (A_n/233)} \times 100 \quad (1)$$

Sulfur content was investigated by X-ray photoelectron spectroscopy using Mg K_α excitation. Charging of insulating films was minimised by use of an electron flood gun, and any remaining charging effects were counteracted by offsetting the energy scale with respect to the known values for carbon peaks. The absolute values for the sulfur content (*i.e.* S : C ratio) of the films were calculated by comparison of the areas of selected S peak(s) and C peak(s), following calibration using the sensitivity factors[28] appropriate for each element.

The resistivity of the films was determined by four-point probe[29] measurements. Being a technique that relies upon surface contacts, this will measure the surface conductivity of diamond, rather than the conductivity through the bulk. Care was therefore taken to ensure that the surface properties of each of the diamond samples were treated identically both during and after deposition.

(b) Optical emission spectroscopy

Optical emission spectra were obtained using an Oriel InstaSpec IV spectrometer to disperse emission from the plasma after exiting through a quartz view port, focusing and passage through a quartz fibre-optic bundle. Light was sampled from the center of the plasma ball with a spatial resolution of ~3 mm, and a spectral resolution ~0.9 nm, over the wavelength range of 200–520 nm.

(c) Molecular beam mass spectrometry. A full description of the MBMS system and gas sampling technique has been published previously,[17] but a brief outline will be given here. A two stage differential pumping system was used to sample gas (at 20 Torr) from the side of the microwave plasma ball *via* an orifice (~100 μm diameter) in a sampling cone. Although such an intrusive method is bound to perturb the plasma, the fact that the position of the plasma ball and the reflected microwave power level are insensitive to the presence of the probe, suggests that this perturbation is minimal. However, the presence of the probe does reduce the size of the plasma ball at pressures above 20 Torr, thus making measurements at the growth pressure of 40 Torr unreliable. Therefore MBMS measurements were carried out at the lower pressure of 40 Torr. Gas passing through this orifice experienced a pressure differential ($20 \rightarrow 10^{-3}$ Torr) and underwent adiabatic expansion, forming a molecular beam in which chemical reactions were effectively frozen out. The molecular beam then passed through a collimating skimmer into a quadrupole mass spectrometer (Hiden Analytical) maintained at ~10^{-6} Torr, whereupon gas phase species were ionized by electron impact.

The electron ionisation energy is user-selectable in the range 4–70 eV. The electron ioniser energies used to detect each species were: CH_4, CO, CS_2, SO and SO_2 16.0 eV, C_2H_2 13.2 eV (to minimise contributions to the $m/z = 26$ signal due to the cracking of C_2H_4 occurring above 13.5 eV), H_2S 13.2 eV, CS 13.6 eV (to minimise signal from CO_2 occurring above 13.8 eV), CH_3 13.6 eV (to reduce signal from cracking of CH_4 above 14.3 eV), S_2 12.0 eV (to minimise contributions to the $m/z = 64$ signal due to ionisation of SO_2 occurring above 12.35 eV) and S 13.2 eV (to reduce cracking of S_2 and CS_2 which occurs above 14.0 eV).

As stated previously,[21] it has proved impossible to convert the counts measured by the MBMS into absolute mole fractions when using CH_4/CO_2 plasmas. In order to obtain such

a calibration, information is required about: (i) the thermal diffusion coefficients for species of different masses within the plasma bulk; (ii) the relative transmission efficiency of the sampling orifice for heavy and light particles; and (iii) the detector sensitivity factors for different species. Although estimates for some of these data can be obtained, we lack sufficient information about all of the important species to make conversion of counts into absolute mole fractions reliable. Therefore, no correction has been attempted for these effects, which may result in the experiment being more sensitive to lighter species (*e.g.* CH_4) than heavier species (*e.g.* CS_2).

As a consequence of the experimental considerations made above, no quantitative comparisons of species counts will be made, and the quoted magnitude of signal counts should be treated with caution. Instead, this work will concentrate on comparisons of the trends observed in measured species counts over the range of plasma gas mixtures investigated.

(d) Computer simulation. Computer simulations of the gas phase reactions occurring in the microwave plasma were carried out using the SENKIN code, which is part of the CHEMKIN package.[30] All of the C, H and O containing species reactions and temperature dependent rate constants used in these calculations were obtained from the GRI-Mech 3.0 reaction mechanism database,[31] as used for previous studies of H/C/O gas mixtures.[32] Information regarding reactions involving C, H and S containing species was obtained from the literature, with rate data for analogous O containing species reactions used when none for S were available. A more detailed description of the H/C/S reaction mechanism, its implementation and validation, is presented elsewhere.[33] The remaining H, C, O and S containing species reactions were obtained from the Leeds University combined methane and SO_x combustion mechanism[34] which, although being the least reliable aspect of the reaction mechanism used during the present SENKIN simulations, has been tested against a wide variety of data.[35]

Mole fractions of the 53 gas phase species (H_2, H, CH_4, CH_3, CH_2, CH, C_2H, C_2H_2, C_2H_3, C_2H_4, C_2H_5, C_2H_6, O_2, O, OH, H_2O, HO_2, H_2O_2, CO, CO_2, CH_2O, CH_2OH, CH_3O, CH_3OH, CH_2CO, CH_2HCO, C, HCO, HCCO, HCCOH, S_2, S, SH, H_2S, HS_2, H_2S_2, H_2SO, SO, SO_2, SO_3, HSO, HSOH, HSO_2, HOSO, $HOSO_2$, CS, CS_2, COS, HOSHO, CH_3SH, CH_3S, CH_2S and HCS) involved in this reaction scheme were calculated, for a chosen input gas mixture (*e.g* 1% H_2S/51% CH_4/49% CO_2), at a fixed gas temperature, T_{gas}, and pressure (20 Torr). Limitations inherent in this approach include:

1. The adoption of a single temperature, *e.g.* 2000 K, which is considered to be representative of the gas temperature of a 51% CH_4/49% CO_2 plasma in low power (<3 kW) microwave CVD chambers at ~20 Torr, within the region from which gas was sampled during MBMS measurements.[36]
2. The neglect of any electron impact dissociation, ionic reactions or surface chemistry. The modelling assumes that reaction is initiated solely by thermal dissociation.
3. Transport into and out of the reaction volume neglected also. To mimic experiment, therefore, it is necessary to run the simulation for a finite (user selected) time, t. The calculations reported here employ $t = 5$ s. This time was previously found to give the best agreement with MBMS measured trends in CO_2/CH_4 plasma species counts.[36]

Calculations were run repeatedly in order to determine plots of species mole fraction as functions of gas mixing ratio.

III. Results and discussion

(a) Film growth

Fig. 1 presents SEM images of diamond films grown at substrate temperatures of (a)–(c) 620 °C and (d)–(f) 900 °C, at various H_2S additions. The film grown at the lower T_{sub}, using an H_2S addition of 100 ppm (Fig. 1(a)) exhibits a continuous coating of predominantly triangular facets ~5 μm in size. Increasing H_2S input levels to 2000 ppm decreases the facet size to <2.5 μm (Fig. 1(b)), while 5000 ppm H_2S additions produce a film primarily composed of small (<1 μm) facets (Fig. 1(c)) with the occasional larger crystallite. In contrast, there is little change in the surface morphology of films grown at $T_{sub} = 900$ °C for H_2S additions of 100, 2000 and 5000 ppm, as illustrated by Figs. 1(d), (e) and (f), respectively. Here, all three films are continuous and display crystalline facets ~5 μm in size.

Fig. 2 shows that the growth rates of films grown at $T_{sub} = 900$ °C are approximately one order of magnitude

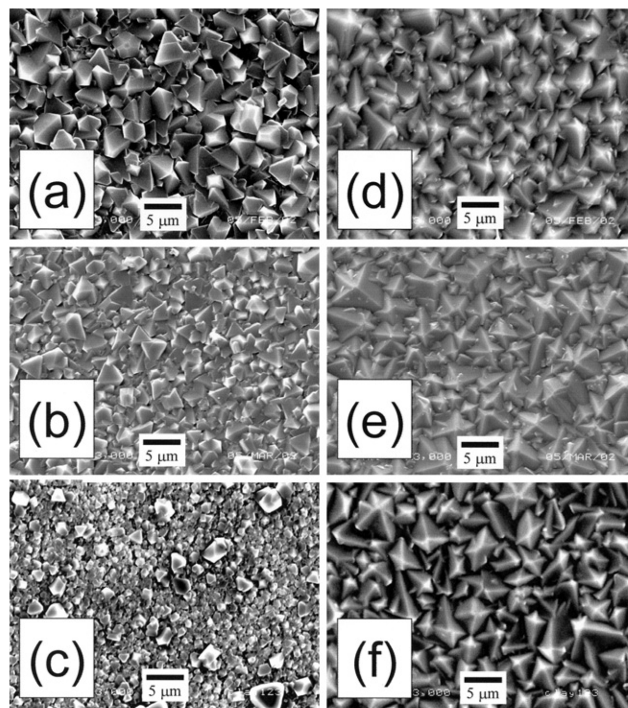

Fig. 1 SEM micrographs for films grown using 51% CH_4/49% CO_2 gas mixtures and T_{sub} of 620 °C with H_2S additions of (a) 100, (b) 2000 and (c) 5000 ppm, and $T_{sub} = 900$ °C with H_2S additions of (d) 100, (e) 2000 and (f) 5000 ppm in a MW plasma reactor. Conditions: total gas flow 200 sccm, growth time 8 h, pressure 20 Torr, 1 kW applied microwave power.

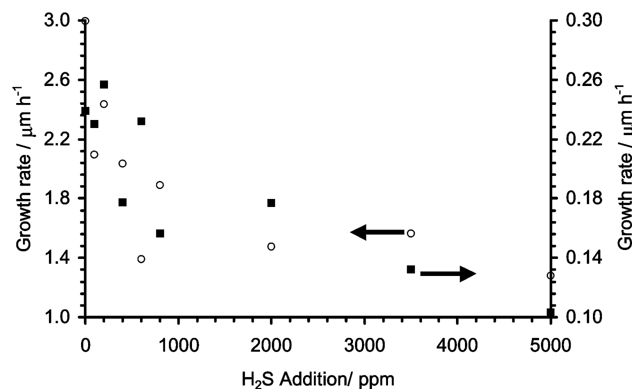

Fig. 2 Film growth rate (measured by cross-sectional SEM), *versus* H_2S addition for films grown in H_2S/51% CH_4/49% CO_2 gas mixtures at two substrate temperatures. Key: (■) $T_{sub} = 620$ °C, (○) $T_{sub} = 900$ °C, with other process conditions as for Fig. 1. Both data sets show a ~66% reduction in growth rate over the range of H_2S addition shown.

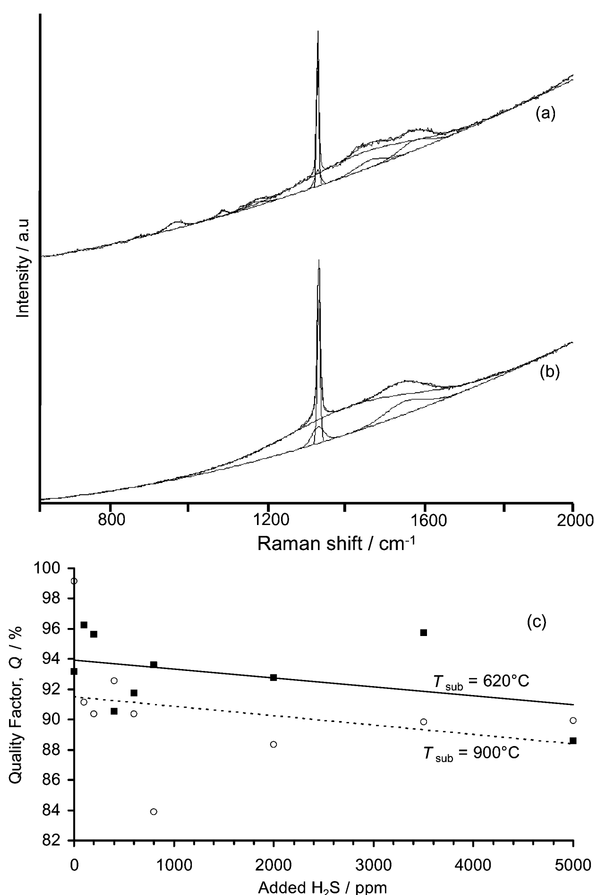

Fig. 3 Laser Raman spectra of films deposited using 5000 ppm H_2S/51% CH_4/49% CO_2 gas mixtures for (a) $T_{sub} = 620\,°C$ and (b) $T_{sub} = 900\,°C$. Each spectrum includes a fitted baseline and Gaussian line shape curve fits. Fig. 3(c) presents a plot of the diamond film quality factor, Q, *vs.* H_2S addition (Q having been defined in eqn. (1)). Key: (■) $T_{sub} = 620\,°C$, (○) $T_{sub} = 900\,°C$, with other process conditions as for Fig. 1. The lines are linear least squares fits to the two data sets (as labeled).

greater than for those grown at 620 °C. However, despite this difference, the observed growth rate trend, *i.e.* a fall of ~66% when H_2S addition is increased from 0 to 5000 ppm, is similar for both temperatures.

Raman spectra of diamond films grown at an H_2S addition of 5000 ppm at (a) 620 °C and (b) 900 °C are presented in Figs. 3(a) and (b). Both spectra can be fitted using a quadratic base line, two Gaussian peaks centered at ~1332 cm^{-1} (sharp diamond Raman line and a broader D band), a peak at ~1530 cm^{-1} (the G band) and a broad band at ~1450 cm^{-1} (polyacetylene[37] or a diamond precursor[38]). However, a number of additional features are evident in the spectrum of the sample grown at the lower T_{sub}, including the presence of peaks at ~1172 cm^{-1} (nanophase diamond[39] or polyacetylene present in grain boundaries[37]) and 876, 967 and 1088 cm^{-1}. These additional peaks may correspond with nanoscale sp^3 phases resulting from the small sized crystallites grown at this low T_{sub}.

In order to gain a measure of film quality (*i.e.* the ratio of $sp^3:sp^2$ carbon bonding) the quality factor, Q (as defined in eqn. (1)) is presented in Fig. 3(c). Somewhat surprisingly, Q for films grown at the lower T_{sub} is generally slightly higher than those deposited at 900 °C. In both cases there is a slight fall in film quality with increased H_2S addition for both sets of data.

XPS analysis has afforded S/C ratios of high temperature films grown with input gas mixture H_2S concentrations of

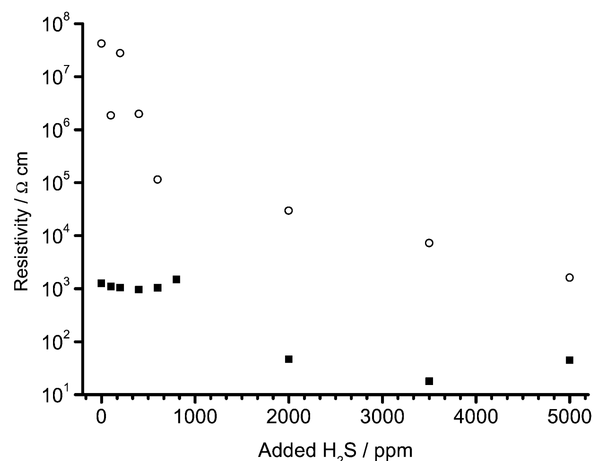

Fig. 4 Four point probe resistivity *vs.* H_2S addition for films deposited using H_2S/51% CH_4/49% CO_2 gas mixtures. Key: (■) $T_{sub} = 620\,°C$, (○) $T_{sub} = 900\,°C$, with other process conditions as for Fig. 1.

3500 ppm (S/C ~0.07%) and 5000 ppm (S/C ~0.08%). We note that XPS yields an average signal over the whole area of the substrate (1 cm^2), and so the position of the S (*i.e.* grain boundaries *versus* crystallites) cannot be determined. S/C ratios for all other deposited films were below the detection limit of the apparatus (~0.05%). It should be noted that these measured film S/C ratios are generally an order of magnitude lower than that of the input gas mixture (*e.g.* input S/C ratio = 0.5% in the case of an H_2S addition level of 5000 ppm).

There is a general fall in resistivities with increased H_2S addition, for the films grown at both high and low T_{sub} (Fig. 4). The scatter seen for samples grown with low H_2S additions and at high T_{sub} is due to the measurements being made at the limit of the apparatus capabilities. There is also a large offset of ~3 orders of magnitude between resistivity measurements of high and low T_{sub} grown films. Apart from this offset, the trend in film resistivities for H_2S additions over 1000 ppm is similar for both datasets. Both show a ~100-fold reduction in resistivity when H_2S additions are increased from 1000 to 5000 ppm.

(b) Optical emission spectroscopy

An optical emission spectrum of a 1% H_2S/51% CH_4/49% CO_2 MW plasma is presented in Fig. 5(a). Emissions due to C_2 Swan bands are clearly present at ~470, 516 and 560 nm. Also evident are emissions of the 3rd Positive and 5B bands (260–370 nm) and Angstrom bands (~451, 484, 520 and 561 nm) of CO. Emissions due to CH (431 nm) and H (483 nm) are also seen. Emission spectra taken of plasmas containing 0% and 1% H_2S were almost identical. Therefore, six emission wavelengths were chosen and their relative intensities were plotted *vs.* H_2S addition, as presented in Fig. 5(b). It is clear that the intensities of the CO and H emission features stay relatively constant or even increase slightly over the range of H_2S additions, while those of C_2 and CH are seen to reduce by ~18 and 20%, respectively, over the same range. This suggests that increased H_2S addition to the 51% CH_4/49% CO_2 gas mixture causes a reduction in hydrocarbon concentrations.

(c) Computer simulation and MBMS. Fig. 6 shows combined plots of MBMS measured species counts and SENKIN predicted species mole fractions, against added H_2S. The respective vertical scales in each plot have been arranged so as to aid comparison. The plots of C_2H_2, CH_4 and CH_3 show good agreement between the measured and predicted species trends, with H_2S addition resulting in a decrease in species

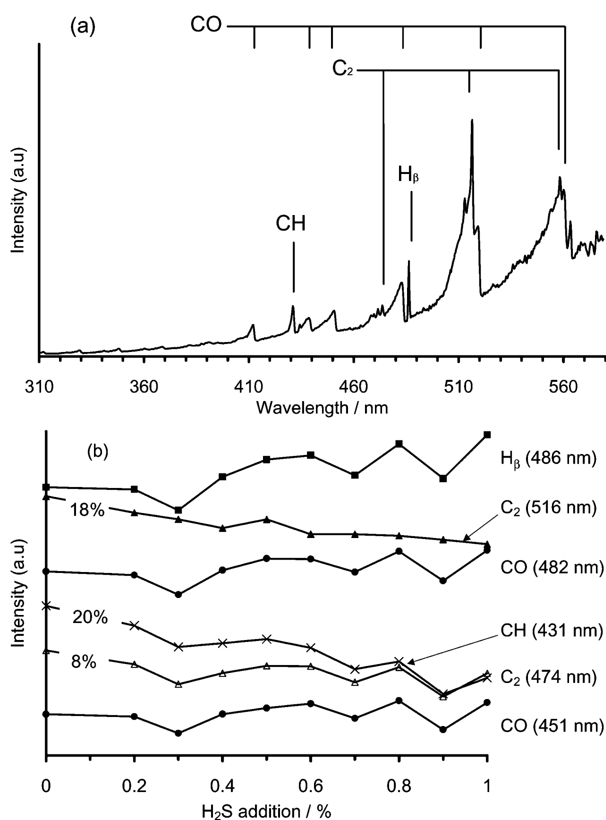

Fig. 5 Plot of (a) optical emission spectrum of a 1% H_2S/51% CH_4/49% CO_2 MW plasma and (b) peak intensity *vs.* H_2S addition to a 51% CH_4/49% CO_2 gas mixture. Emission features are as labeled and percentages given indicate the drop in intensity of the indicated feature over the range of H_2S addition shown. Conditions: applied microwave power 1 kW, pressure 40 Torr.

mole fraction and measured counts. Similarly, experiment and simulation are in agreement in the case of H_2S, CS and CS_2, with species mole fraction and measured counts increasing upon increased H_2S addition. There is, again, good agreement between MBMS and SENKIN results in the case of SO. However, the predicted mole fraction, X, of SO is $\sim 10^{-7}$, which is ~ 100 times below the estimated detection limit of the MBMS apparatus. This suggests that SO is present within the microwave plasma at concentrations much greater than predicted by SENKIN. A similar conclusion can be drawn from the SENKIN and MBMS results for SO_2. Here, the scatter in SO_2 measured species counts data suggests SO_2 concentrations are near the MBMS detection limit ($X \sim 10^{-5}$), whereas the predicted SO_2 mole fractions are below this, *i.e.* $\sim 10^{-11}$. On the other hand, the MBMS measured counts of S and S_2 appear to be at or below the MBMS detection limit, suggesting that the predicted mole fractions of S ($\sim 10^{-4}$) and S_2 ($\sim 10^{-5}$) may be overestimates.

IV. Discussion

H_2S addition to 51% CH_4/49% CO_2 MW plasmas during diamond CVD is seen to have a considerable impact upon the growth rates, quality and resistivities of the resulting films. S addition also induces changes in film morphology, particularly in the case of low temperature deposition, *e.g.* $T_{sub} = 620\,°C$. Reduction of T_{sub} from 900 to 620 °C results in a $\sim$10-fold drop in film growth rate. Such reduction in growth rates upon lowering of T_{sub} is consistent with previous observations,[21–23] but the increased substrate–plasma separation used during low T_{sub} deposition in the present studies may also contribute to the observed variation. However, the fact that we observe very similar downward trends in film growth rate for increased H_2S additions at both deposition temperatures suggests that the trend is primarily due to gas phase reaction instigated by H_2S, rather than gas–surface interactions.

A large offset was observed between the measured film resistivities of samples grown at high (900 °C) and low (620 °C) T_{sub}. We suggest that the lower resistivity of the low temperature grown samples is probably due to H-induced surface conduction.[40–43] This effect is reported to be annealed out of films at temperatures above $\sim$700 °C in vacuum and $\sim$190 °C in air.[42] The resistivity of such annealed films is several orders of magnitude greater than the H-terminated samples, pre-annealing. We therefore suspect that the growing diamond surface is (at least partially) H-terminated at $T_{sub} = 900\,°C$. However, at the end of a deposition run the plasma is shut off and the film is left to cool down in a 100% CO_2 atmosphere. During cooling from 900–700 °C, we envisage that the H-induced surface conductivity is annealed out, thereby resulting in the highly resistive film observed. $T_{sub} = 620\,°C$ is below the temperature for such annealing. In this scenario, therefore, films grown at this lower substrate temperature would retain their H-induced surface conductivity intact when cooled in a CO_2 atmosphere. Previously films have been deposited at $T_{sub} = 900\,°C$ using a MW reactor (identical to that used in the present study) and H_2S/1% CH_4/H_2 gas mixtures.[10] After growth, these films were cooled in a H_2 atmosphere and the measured film resistivities were comparable with those obtained for the low temperature deposited films in the present work. This observation lends further credence to the scenario outlined above.

Increased H_2S additions (>1000 ppm) appear to cause a reduction in film resistivities, regardless of T_{sub}. It is important to note that the reduction in film resistivities observed between high T_{sub} grown films with 0 and 5000 ppm H_2S additions is much greater than the $\sim$3-fold reduction seen for H_2S doping of 1% CH_4/H_2 gas mixtures ($\sim$3 times reduction), using similar process conditions.[10,11] However, it remains unclear whether this reduction is a result of S-incorporation into the diamond films or due to an increase in graphitic phases within the film (as indicated by a parallel reduction in the quality factor).

OES measurements of C_2 and CH emission features suggest that increased H_2S additions caused a drop in gas phase hydrocarbon concentrations. This conclusion is reinforced by the observed trends in MBMS measured counts and SENKIN predicted mole fractions for C_2H_2, CH_4, and CH_3. The methyl radical is generally believed to be the major diamond growth precursor in most low pressure CVD reactors.[44,45] It therefore seems reasonable to associate the measured drop in CH_3 MBMS counts with the observed drop in film growth rates upon increased H_2S addition.

A reaction scheme for the chemistry of H_2S addition to 51% CH_4/49% CO_2 gas mixtures is presented in Table 1. It should be noted that all except Reaction 4 are composite conversions composed of many elementary reactions. Reaction 1 is the dominant reaction involving S containing species. This is shown by the large SENKIN predicted mole fractions and MBMS measured counts of CS_2 and CS. Previous investigations of 50% CH_4/50% CO_2 gas mixtures[21] concluded that the majority of the input carbon is transformed to CO *via* Reaction 2. Any excess CH_4 not destroyed by this reaction is able to undergo further conversions to produce C_2H_2 and CH_3, *via* Reactions 3 and 4, respectively. However, Reaction 1 is able to compete with these reactions, with the result that increased H_2S additions leading to a reduction in the CH_4 available for production of C_2H_2, CH_3 and H_2O. This is analogous to the situation seen for H_2S addition to 1% CH_4/H_2

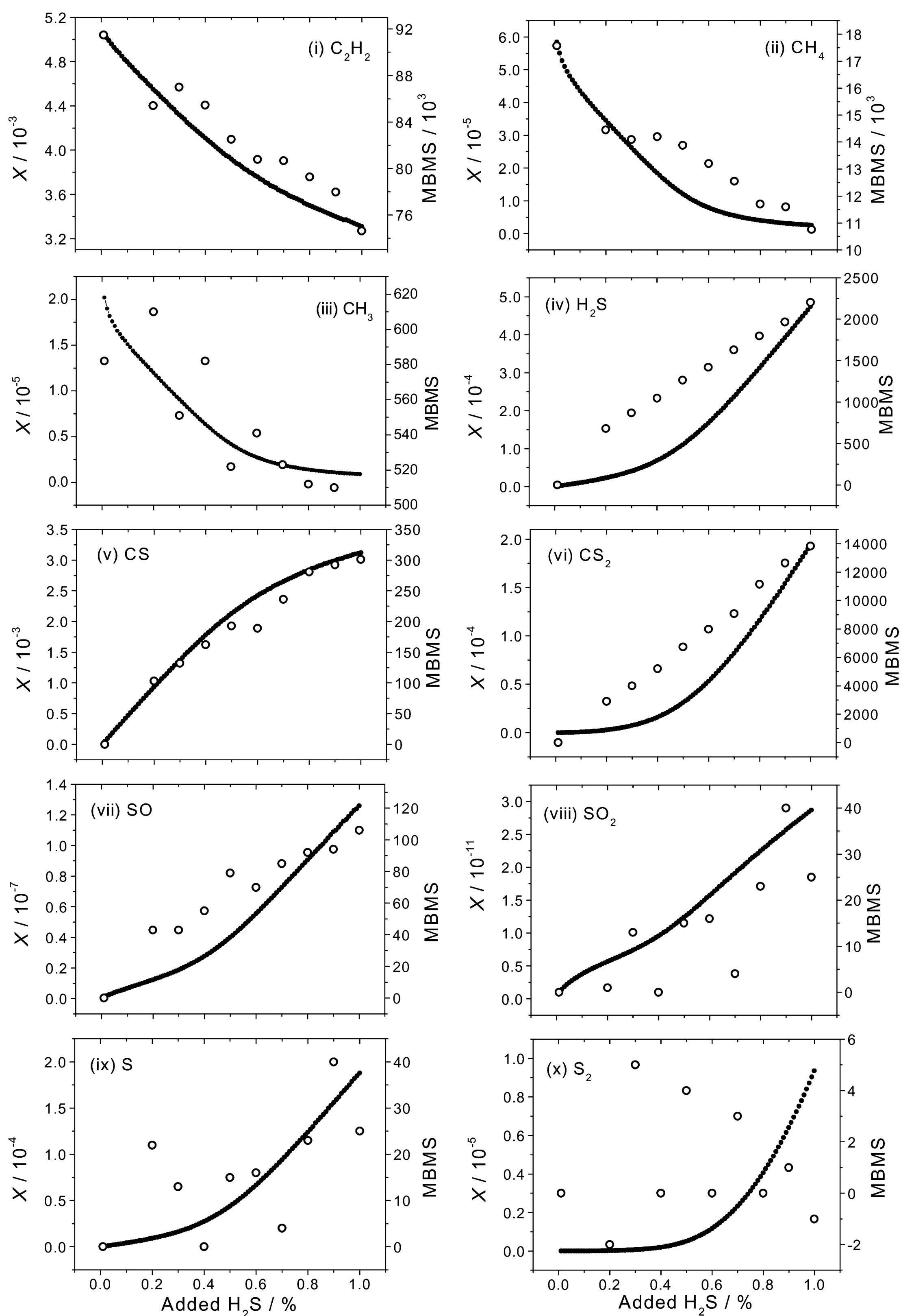

Fig. 6 Plots of MBMS measured species counts (right hand scale) and SENKIN predicted species mole fractions (left hand scale) *vs.* H_2S addition to a 51% CH_4/49% CO_2 gas mixture, for the following species: (i) C_2H_2; (ii) CH_4; (iii) CH_3; (iv) H_2S; (v) CS; (vi) CS_2; (vii) SO; (viii) SO_2; (ix) S and (x) S_2. Conditions are as given in Fig. 2, except that the pressure was reduced to 20 Torr to improve plasma stability in the presence of the sampling probe. SENKIN computer simulation results are for a H_2S/51% CH_4/49% CO_2 gas mixture at a temperature of 2000 K and a pressure of 20 Torr. Key: ○ MBMS species counts, (●) SENKIN computer simulation mole fractions. The two data sets in each panel have been vertically scaled to illustrate the degree of consistency between the experimental and modeled trends.

Table 1 Proposed reaction scheme for the gas phase chemistry of $H_2S/51\%\ CH_4/49\%\ CO_2$ diamond CVD gas mixtures at 2000 K and ~20 Torr. ΔG_{reac} values were calculated using species Gibbs free energies of formation obtained from ref. 48 and were also used to calculate reaction equilibrium constants, K_{eq}

	Reaction	ΔG_{reac}/kJ mol^{-1}	K_{eq}
1	$CH_4 + 2H_2S \leftrightharpoons CS_2 + 4H_2$ [a]	−172.1	3.124×10^4
2	$CO_2 + CH_4 \leftrightharpoons 2CO + 2H_2$ [b]	−306.0	1.014×10^8
3	$2CH_4 \leftrightharpoons C_2H_2 + 2H_2$ [b]	−144.4	5.916×10^3
4	$CH_4 + H \leftrightharpoons CH_3 + H_2$	−53.30	24.67
5	$CO_2 + H_2 \leftrightharpoons CO + H_2O$ [b]	−25.00	5.477
6	$CO_2 + H_2S \leftrightharpoons CO + H_2 + SO$	32.45	1.420×10^{-1}
7	$H_2O + H_2S \leftrightharpoons SO + 2H_2$	60.74	2.592×10^{-2}
8	$CO_2 + SO \leftrightharpoons CO + SO_2$	−36.34	8.893

[a] Reaction taken from ref. 10. [b] Reaction taken from ref. 21.

gas mixtures.[10] As stated above, the reduction in CH_3 concentrations caused by increased H_2S addition leads to a reduction in deposited film growth rates.

In addition, we recall that there is a large (~2 mm) separation between the visible edge of the plasma and the substrate in the case of films grown at low T_{sub} grown films, whereas the growth surface of samples deposited at high T_{sub} are in direct contact with the visible edge of the plasma. The larger substrate–plasma separation for low T_{sub} grown films clearly causes a further reduction in the CH_3 flux reaching the substrate surface, as a result of radical recombination reactions (*e.g.* involving CH_3 and H radicals). Arguably of even greater importance, is the reduced diffusion of species across the growing film surface at low T_{sub}.[23,46,47] Such diffusion is considered necessary for the growth of uniform diamond CVD films, as carbon containing species move to step edges allowing ordered crystal growth. These two effects are likely to be responsible for the much greater change in deposited film surface morphology observed upon H_2S addition at lowered T_{sub}, compared to growth at the higher T_{sub}.

Table 1 also sets out two possible routes to the production of SO (Reactions 6 and 7). The first involves a composite reaction between CO_2 and H_2S producing CO, H_2 and SO, while in the second reaction H_2O and H_2S react to form SO and hydrogen. At 2000 K, the Gibbs free energy for both reactions, ΔG_{reac}, is greater than zero, indicating that at equilibrium the reverse of the reactions as written are spontaneous (*i.e.* $\Delta G_{reac} < 0$).

However, as stated previously, the MBMS measurements suggest that the SENKIN calculations underestimate the true SO and SO_2 concentrations. This might reflect an overestimation of the forward rate constant of one or more of the elementary reactions of which Reaction 1 is comprised,[33] which would result in a reduced concentration of H_2S available to participate in Reactions 6 and 7, and thus a lower predicted SO mole fraction. This, in turn, would cause an underestimation of the predicted mole fraction of SO_2 produced *via* Reaction 8. Alternatively, or additionally, it may reflect inadequacies in the kinetic data for S/O and H containing species reactions that we have taken from the Leeds combined methane and SO_x combustion mechanism.[34] The fact that some 70% of these rate constants are either estimations or extrapolations from lower temperatures[35] serves to underline the inadequacy of the database of reactions involving H/C/O/S containing species.

Previous studies have proposed that S-incorporation into films occurs *via* the CS radical.[10,11] On that basis, we suggested[33] that since both CS and CH_3 are thought necessary for S incorporation and diamond growth, respectively, a parameter defined as the product of SENKIN predicted mole fractions of these two species, $[CH_3] \times [CS]$, might be a useful predictor for S incorporation into good quality CVD diamond films. We previously suggested[36] that a ratio of $[H]/[C_2H_2] > 0.2$ is an additional prerequisite for the deposition of good quality diamond. This requirement is met for all gas mixtures investigated in the present work.

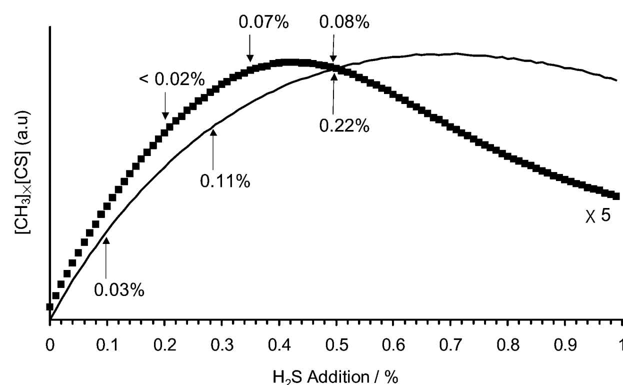

Fig. 7 Plots of $[CH_3] \times [CS]$ *vs.* H_2S addition to 1% CH_4/H_2 ($T_{gas} = 1630$ K) and 51% CH_4/49% CO_2 ($T_{gas} = 2000$ K) gas mixtures obtained from the SENKIN calculations. Conditions: pressure 40 Torr, reaction time 5 s. The magnitude of the product $[CH_3] \times [CS]$ is proposed as a reasonable predictor of the ability of a gas mixture to produce diamond films with high S-incorporation. The numbers present the S/C ratio (as measured by XPS) for films deposited at the H_2S additions indicated. Key: (—) H_2S/1% CH_4/H_2 gas mixture, (■) H_2S/51% CH_4/49% CO_2 gas mixture (scaled up by a factor of 5).

The S incorporation parameter, $[CH_3] \times [CS]$, is plotted in Fig. 7 as a function of H_2S addition to both 1% CH_4/H_2 and 51% CH_4/49% CO_2 gas mixtures. It should be noted that the SENKIN product for the 51% CH_4/49% CO_2 gas mixture has been scaled vertically by a factor of five to fit onto the plot. XPS measured S/C ratios for films deposited using these gas mixtures (at $T_{sub} = 900\,°C$) are indicated also. The figure illustrates the point that for a given H_2S addition, 1% CH_4/H_2 gas mixtures are found to yield films with higher S/C ratios than 51% CH_4/49% CO_2 mixtures. Such an observation is consistent with the smaller SENKIN predicted values of $[CH_3] \times [CS]$ calculated for the latter gas mixture. Indeed, this parameter is seen to maximise in the case of the H_2S/51% CH_4/49% CO_2 gas mixtures, at ~0.42% added H_2S. This is midway between the only two H_2S addition values (0.35 and 0.5%) at which the S content was measurable by XPS.

V. Conclusions

Diamond films have been grown from 51% CH_4/49% CO_2 gas mixtures, with H_2S additions of up to 5000 ppm, and at substrate temperatures of 900 and 620 °C. The texture of films grown at the higher T_{sub} is seen to be independent of the level of H_2S addition while the morphology of films deposited at the lower T_{sub} are greatly influenced by increased H_2S additions. The growth rate, quality and resistivity of deposited films are all reduced by increased H_2S additions. Gas phase experimental species number density measurements and companion SENKIN computer simulations allow construction of a plausible reaction scheme for the chemistry of H_2S/51% CH_4/49% CO_2 gas mixtures.

Acknowledgements

The authors would like to thank the EPSRC for project funding and De Beers Industrial Diamond for financial support (JRP). Thanks also go to Sean Pearce and the Bristol Interface Analysis Centre for XPS work, Drs. Colin Western,

Jason Riley, Dudley Shallcross and Jeremy Harvey, and Anella Seddon, all in the School of Chemistry at Bristol, for their many and varied contributions to aspects of this work.

References

1 K. E. Spear, J. P. Dismukes, *Synthetic Diamond—Emerging CVD Science and Technology*, Wiley, New York, 1994.
2 P. W. May, *Philos. Trans. R. Soc. Lond., Ser. A*, 2000, **358**, 473.
3 B. V. Spitsyn, L. L. Bouilov and B. V. Derjaguin, *J. Cryst. Growth*, 1981, **52**, 219.
4 K. Okano, *Diamond: Electronic properties and applications*, Kluwer Academic Publishers, Dordrecht, 1995.
5 M. Hasegawa, D. Takeuchi, S. Yamanaka, M. Ogura, H. Watanabe, N. Kobayashi, H. Okushi and K. Kajimura, *Jpn. J. Appl. Phys.*, 1999, **38**, L1519.
6 I. Sakaguchi, M. N. Gamo, Y. Kikuchi, E. Yasu and H. Haneda, *Phys. Rev. B*, 1999, **60**, R2139.
7 M. N. Gamo, E. Yasu, C. Xiao, Y. Kikuchi, K. Ushizawa, I. Sakaguchi, T. Suzuki and T. Ando, *Diamond Relat. Mater.*, 2000, **9**, 941.
8 M. N. Gamo, C. Xiao, Y. Zhang, E. Yasu, Y. Kikuchi, I. Sakaguchi, T. Suzuki, Y. Sato and T. Ando, *Thin Solid Films*, 2001, **382**, 113.
9 R. Kalish, A. Reznik, C. Uzan-Saguy and C. Cytermann, *Appl. Phys. Lett.*, 2000, **76**, 757.
10 J. R. Petherbridge, P. W. May, G. M. Fuge, G. F. Robertson, K. N. Rosser and M. N. R. Ashfold, *J. Appl. Phys.*, 2002, **91**, 3605.
11 J. R. Petherbridge, P. W. May, G. M. Fuge, K. N. Rosser and M. N. R. Ashfold, *Diamond Relat. Mater.*, 2002, **11**, 301.
12 H. Sternschulte, M. Schreck and B. Strizker, *Diamond Relat. Mater.*, 2002, **11**, 296.
13 C. A. Rego, P. W. May, C. R. Henderson, M. N. R. Ashfold, K. N. Rosser and N. M. Everitt, *Diamond Relat. Mater.*, 1995, **4**, 770.
14 R. S. Tsang, C. A. Rego, P. W. May, J. Thumin, M. N. R. Ashfold, K. N. Rosser, C. M. Younes and M. J. Holt, *Diamond Relat. Mater.*, 1996, **5**, 359.
15 C. A. Rego, R. S. Tsang, P. W. May, M. N. R. Ashfold and K. N. Rosser, *J. Appl. Phys.*, 1995, **79**, 7264.
16 R. S. Tsang, P. W. May, M. N. R. Ashfold and K. N. Rosser, *Diamond Relat. Mater.*, 1998, **7**, 1651.
17 S. M. Leeds, P. W. May, E. Bartlett, M. N. R. Ashfold and K. N. Rosser, *Diamond Relat. Mater.*, 1999, **8**, 1377.
18 S. M. Leeds, P. W. May, M. N. R. Ashfold and K. N. Rosser, *Diamond Relat. Mater.*, 1999, **8**, 226.
19 G. D. Barber and W. A. Yarbrough, *J. Am. Ceram. Soc.*, 1997, **80**, 1560.
20 D. S. Dandy, *Thin Solid Films*, 2001, **381**, 1.
21 J. R. Petherbridge, P. W. May, S. R. J. Pearce, K. N. Rosser and M. N. R. Ashfold, *J. Appl. Phys.*, 2001, **89**, 1484.
22 C. F. Chen, S. H. Chen, H. W. Ko and S. E. Hsu, *Diamond Relat. Mater.*, 1994, **3**, 443.
23 J. Stiegler, T. Lang, M. Nygard-Ferguson, Y. von Kaenel and E. Blank, *Diamond Relat. Mater.*, 1996, **5**, 226.
24 T. Ando, private communication.
25 J. Petherbridge, P. W. May, S. R. J. Pearce, K. N. Rosser and M. N. R. Ashfold, *Diamond Relat. Mater.*, 2001, **10**, 393.
26 *GRAMS/32 User Guide V4.0*, Galactic Industries Corporation, Salem, 2001.
27 S. R. Sails, D. J. Gardiner, M. Bowden, J. Savage and D. Rodway, *Diamond Relat. Matter.*, 1996, **5**, 589.
28 *Handbook of X-ray Photoelectron Spectroscopy*, ed. J. Chastain, Perkin-Elmer, Minnesota, 1992.
29 S. M. Sze, *Physics of Semiconductor Devices*, Wiley, New York, 1981.
30 R. J. Kee, F. M. Rupley and J. A. Miller, Sandia National Laboratories Report SAND89-8009B, 1989.
31 G. P. Smith, D. M. Golden, M. Frenklach, N. W. Moriarty, B. Eiteneer, M. Goldenberg, C. T. Bowman, R. K. Hanson, S. Song, W. C. Gardiner, Jr., V. V. Lissianski, Z. Qin, http://www.me.berkeley.edu/gri_mech/.
32 J. R. Petherbridge, P. W. May and M. N. R. Ashfold, *J. Appl. Phys.*, 2001, **89**, 5219.
33 J. R. Petherbridge, P. W. May, D. E. Shallcross, J. N. Harvey, G. M. Fuge, K. N. Rosser and M. N. R. Ashfold, *Diamond Relat. Mater.*, 2002, submitted.
34 K. J. Hughes, A. S. Tomlin, E. Hampartsoumian, http://www.chem.leeds.ac.uk/Combustion/combine.htm.
35 K. J. Hughes, A. S. Tomlin, V. A. Dupont and M. Pourkashanian, *Faraday Discuss.*, 2001, **119**, 337.
36 M. N. R. Ashfold, P. W. May, J. R. Petherbridge, K. N. Rosser, J. A. Smith, Y. A. Mankelevich and N. V. Suetin, *Phys. Chem. Chem. Phys.*, 2001, **3**, 3471.
37 A. C. Ferrari and J. Robertson, *Phys. Rev. B*, 2001, **63**, 121 405(R).
38 V. Vorlicek, J. Rosa, M. Vanecek, M. Nesladek and L. M. Stals, *Diamond Relat. Matter.*, 1997, **6**, 704.
39 W. A. Yarbrough and R. Messier, *Science*, 1990, **247**, 688.
40 M. I. Landstrass and K. V. Ravi, *Appl. Phys. Lett.*, 1989, **55**, 975.
41 H. J. Looi, M. D. Whitfield, J. S. Foord and R. B. Jackmann, *Thin Solid Films*, 1999, **343**, 623.
42 F. Maier, M. Riedel, B. Mantel, J. Ristein and L. Ley, *Phys. Rev. Lett.*, 2000, **85**, 3472.
43 J. Ristein, F. Maier, M. Riedel, M. Stammer and L. Ley, *Diamond Relat. Mater.*, 2001, **10**, 416.
44 B. J. Garrison, E. J. Dawnkaski, D. Srivastava and D. W. Brenner, *Science*, 1992, **255**, 835.
45 S. J. Harris and D. G. Goodwin, *J. Phys. Chem.*, 1993, **97**, 23.
46 M. Frenklach and S. Skokov, *J. Phys. Chem. B*, 1997, **101**, 3025.
47 K. Larsson and J. O. Carlsson, *Phys. Rev. B*, 1999, **59**, 8315.
48 M. W. Chase, Jr., NIST-JANAF Thermochemical Tables, 4th edn., *J. Phys. Chem. Ref. Data*, 1998, Monograph No. 9.